THE JOURNAL OF BIOLOGICAL CHEMISTRY VOL. 282, NO. 7, pp. 4310–4317, February 16, 2007

LPA_4/GPR23 Is a Lysophosphatidic Acid (LPA) Receptor Utilizing G_s-, G_q/G_i-mediated Calcium Signaling and $G_{12/13}$-mediated Rho Activation*

Received for publication, November 22, 2006 Published, JBC Papers in Press, December 13, 2006, DOI 10.1074/jbc.M610826200

Chang-Wook Lee, Richard Rivera, Adrienne E. Dubin, and Jerold Chun[1]

From the Department of Molecular Biology, Helen L. Dorris Institute for Neurological and Psychiatric Disorders, The Scripps Research Institute, La Jolla, California 92037

Lysophosphatidic acid (LPA) is a bioactive lysophospholipid that signals through G protein-coupled receptors (GPCRs) to produce a range of biological responses. A recently reported fourth receptor, LPA_4/GPR23, was notable for its low homology to the previously identified receptors LPA_{1-3} and for its ability to increase intracellular concentrations of cAMP and calcium. However, the signaling pathways leading to LPA_4-mediated induction of cAMP and calcium levels have not been reported. Using epitope-tagged LPA_4, pharmacological intervention, and G protein mini-genes, we provide independent confirmatory evidence that supports LPA_4 as a fourth LPA receptor, including LPA concentration-dependent responses and specific membrane binding. Importantly, we further demonstrate new LPA-dependent activities of LPA_4 that include the following: receptor internalization; $G_{12/13}$- and Rho-mediated neurite retraction and stress fiber formation; G_q protein and pertussis toxin-sensitive calcium mobilization and activation of a nonselective cation conductance; and cAMP increases mediated by G_s. The receptor is broadly expressed in embryonic tissues, including brain, as determined by Northern blot and reverse transcription-PCR analysis. Adult tissues have increased expression in skin, heart, and to a lesser extent, thymus. These data confirm the identification and extend the functionality of LPA_4 as an LPA receptor, bringing the number of independently verified LPA receptors to five, with both overlapping and distinct signaling properties and tissue expression.

Lysophosphatidic acid (LPA,[2] 1-acyl-2-*sn*-glycerol-3-phosphate) is a water-soluble bioactive phospholipid that can be generated by many cell types and has been shown to influence multiple intracellular signaling pathways, including stimulation of phospholipase C and D, activation of small GTPases, MAPK (mitogen-activated protein kinase), and phosphoinositide 3-kinase (1, 2), and inhibition of adenylyl cyclase (3, 4). LPA signaling through G proteins mediates a variety of biological functions, including cell proliferation, cell survival, cytoskeletal remodeling, cell migration, and alterations in differentiation (3, 5–9). In mice, gene deletion studies of the LPA receptors (10, 11) have shown that LPA receptor-mediated signaling contributes to many other functions in normal and pathological states (12), including vascular and nervous system development (10, 13, 14), female fertility and implantation (15), and the initiation of neuropathic pain (16).

Five LPA-specific GPCRs have thus far been identified, termed LPA_{1-5} (17–22). LPA_4 is the only receptor that has yet to receive independent confirmation as a *bona fide* LPA receptor since its initial report (20). This putative LPA receptor was remarkable for its relatively low predicted amino acid sequence homology compared with the well studied LPA_{1-3}, a K_d ~45 nM for LPA, and an ability to mobilize calcium and increase cAMP production (20). Here we confirm the finding that GPR23 is indeed a biologically relevant receptor for LPA and report several novel aspects of LPA_4 signaling that extend its functional roles.

MATERIALS AND METHODS

Cell Culture and Stable Transfection—B103 neuroblastoma cells and RH7777 hepatoma cells (23) were cultured in Dulbecco's modified Eagle's medium containing 10% heat-inactivated fetal bovine serum (Hyclone, Logan, UT) and antibiotics (Invitrogen). LPA_4-expressing stable cell lines were generated by transfecting B103 cells with linearized HA-tagged mouse LPA_4-pcDNA3.1 (Invitrogen) using Effectene transfection reagent (Qiagen, Valencia, CA). Stable transfectants were selected for by adding 1 mg/ml geneticin (Invitrogen) to the culture media for 2 weeks.

Production of LPA_4 Retrovirus and G Protein Minigenes—HA-tagged mouse and human LPA_4 cDNAs were amplified using the Expand High Fidelity PCR system (Roche Applied Science) using the following primers: 5′-ATGTACCCATACGATGTTCCAGATTACGCTATGGGTGACAGAAGATTTATTG-3′ (forward) and 5′-CTAGAAGGTGGATTCCAGCATT-3′ (reverse). PCR products were subcloned into the pGEM-T Easy T vector (Promega, Madison, WI), and the cDNA insert was sequenced at the The Scripps Research Institute (TSRI) sequencing core facility. The HA-tagged LPA_4 cDNA was subsequently cloned into the NotI site of the LZRS-

* This work was supported by National Institute of Mental Health Grants K02-MH01723 and R01-MH51699 and NINDS Grant R01-NS048478 and NICHD Grant R01-050685 from the National Institutes of Health (to J. C.). The costs of publication of this article were defrayed in part by the payment of page charges. This article must therefore be hereby marked "*advertisement*" in accordance with 18 U.S.C. Section 1734 solely to indicate this fact.

[1] To whom correspondence should be addressed: Dept. of Molecular Biology, The Scripps Research Institute, 10550 North Torrey Pines Rd., ICND-118, La Jolla, CA 92037. Tel.: 858-784-8410; Fax: 858-784-7084; E-mail: jchun@scripps.edu.

[2] The abbreviations used are: LPA, lysophosphatidic acid; GPCR, G protein-coupled receptors; RT, reverse transcription; PTX, pertussis toxin; HA, hemagglutinin; EGFP, enhanced green fluorescent protein; BSA, bovine serum albumin; PBS, phosphate-buffered saline; pF, picofarad.

EGFP Moloney murine leukemia retroviral vector. The Phoenix ecotropic packaging cell line (24) was transfected with the retroviral construct using FuGENE 6 transfection reagent (Roche Applied Science). Retrovirus expression vector (LZRS-EGFP) and Phoenix retrovirus packaging cell lines were provided by Dr. Garry P. Nolan (Stanford University, Stanford, CA). At 48 h post-transfection, retroviral supernatant was filtered through a 0.45-μm filter and frozen in aliquots. Construction of $G_{q/11}$, G_s, G_{12}, and G_{13} minigene retroviruses was described previously (22, 25).

Western Blotting of Membrane Protein Fraction—HA-LPA_4-expressing cells were homogenized in 20 mM Tris buffer, pH 7.5, containing 1 mM EGTA, 1 mM EDTA, and protease inhibitor mixture (Roche Applied Science) using a Dounce homogenizer. The sample was pre-cleared by centrifugation at 2,000 rpm for 5 min at 4 °C. The supernatant was then spun at 15,000 rpm for 90 min. Pellets were resuspended in ice-cold homogenization buffer containing 1% Triton X-100 and then centrifuged at 15,000 rpm for 20 min. The supernatant containing the membrane fraction was separated on a 4–12% SDS-polyacrylamide gel (Invitrogen) under reducing, denaturing conditions and transferred to polyvinylidene difluoride membrane (Millipore, Woburn, MA). HA-tagged LPA_4 receptor expression was detected using an anti-HA antibody (Covance, Berkeley, CA) and horseradish peroxidase-conjugated anti-mouse secondary antibody and visualized with ECL Plus (Amersham Biosciences).

F-actin Detection and Receptor Internalization Assay—Cells were grown overnight on poly-L-lysine-coated 12-mm glass coverslips. The following night, cells were switched to serum-free medium for 16–24 h. The next day, cells were incubated with LPA (1-oleoyl-2-hydroxy-*sn*-glycero-3-phosphate; Avanti Polar-Lipids, Alabaster, AL) for 30 min and then fixed with 4% paraformaldehyde/PBS. Fixed cells were permeabilized in 0.1% Triton X-100/PBS for 15 min and then blocked in 3% BSA/PBS for 30 min. F-actin was visualized by staining with 25 μg/ml rhodamine-phalloidin (Sigma) in PBS/1% BSA for 40 min. Images were acquired using a fluorescence microscope fitted with an AxioCam camera (Carl Zeiss, Thornwood, NY). Receptor internalization was detected by treating serum-starved cells with BSA, LPA, or sphingosine 1-phosphate (Avanti Polar Lipids) for 15 min. Treated cells were then fixed with 4% paraformaldehyde in PBS for 1 h and permeabilized with 0.1% (w/v) Triton X-100 plus 3% BSA in PBS. HA-tagged LPA_4 localization was detected by staining with an anti-HA antibody and Cy3-conjugated anti-mouse IgG secondary antibody (Jackson ImmunoResearch, West Grove, PA) using confocal microscopy (Carl Zeiss, Thornwood, NY).

[^{3}H]LPA Binding to Isolated Membranes—The LPA-binding assay has been described previously by Fukushima *et al.* (23). Briefly, membranes were isolated from transfected RH7777 cells harvested in ice-cold homogenization buffer (20 mM Tris-HCl, pH 7.5) containing 1 mM EDTA and protease inhibitors (Roche Applied Science) and centrifuged at 2,000 rpm for 10 min at 4 °C. The supernatant was then centrifuged at 15,000 rpm for 30 min at 4 °C. 40 μg of membrane fraction was incubated with [^{3}H]LPA (1-oleoyl-[9,10-^{3}H]LPA, 47 Ci/mmol; PerkinElmer Life Sciences) in LPA-binding buffer containing 0.1% fatty acid-free BSA (Sigma) and 0.5 mM $CuSO_4$ for 30 min at room temperature. The [^{3}H]LPA membrane fraction mixture was collected onto a Unifilter 96-GF/B (PerkinElmer Life Sciences). The filter was washed 10 times with binding buffer containing 1% BSA and dried for 30 min at 50 °C. Thirty microliters of MicroScint-O was added to each well of the filter, and radioactivity was measured using a microplate liquid scintillation counter (PerkinElmer Life Sciences). Total and nonspecific binding were evaluated in the absence and presence of 10 μM unlabeled LPA, respectively.

G Proteins and Rho Inhibition in Cultured Cells—To investigate G protein coupling with LPA_4, stable LPA_4-expressing B103 cells were infected with several G protein minigenes and tested 2 days later or treated with PTX (200 ng/ml; List Biological Laboratories, Campbell, CA) for 12 h. To inhibit the Rho pathway, LPA_4-expressing cells were treated with either the Rho inhibitor C3 transferase (10 μg/ml; Cytoskeleton Denver, CO) for 24 h or the ROCK inhibitor Y27632 (10 μM; Calbiochem) for 45 min. Rounded cells were counted following treatment with 1 μM LPA for 30 min in serum-free conditions.

cAMP Measurements—Both acutely infected and stable transfectants expressing LPA_4 were used in these experiments. LPA_4-expressing and control B103 cells were serum-starved overnight in 24-well plates with or without PTX (200 ng/ml; List Biological Laboratories). Following treatment with 0.5 mM 3-isobutyl-1-methylxanthine for 20 min, cells were exposed to LPA (0, 1, 10, and 100 nM and 1 μM) for 30 min with or without forskolin (5 μM). Cells were then lysed in 0.1 N HCl, and cellular cAMP levels were quantified using an enzyme-linked immunosorbent assay-based detection kit (Cayman Chemicals, Ann Arbor, MI) according to the manufacturer's directions.

Determination of Intracellular Calcium Mobilization—B103 cells stably expressing HA-tagged LPA_4 were infected with G protein minigenes 2 days prior to testing and/or exposed to PTX overnight, and control cells were plated on glass coverslips and loaded with Fura-2 acetoxymethyl ester (Fura2-AM) (2.5 μM) for ratiometric calcium imaging studies. Cells lacking LPA_4 expression served as controls. Cells were incubated for 30–60 min at 37 °C in Opti-MEM (Invitrogen) containing Fura2-AM (2.5 μM) and 1.5 μM of pluronic acid (Molecular Probes, Eugene, OR) and then briefly washed with Opti-MEM. Coverslips were perfused with Opti-MEM in a laminar flow perfusion chamber (Warner Instrument Corp., Hamden, CT). LPA (1 μM) was bath-applied by gravity perfusion when indicated. Images of Fura-2-loaded cells with the excitation wavelength alternating between 340 and 380 nm were captured with a cooled CCD camera (Carl Zeiss). The ratio of fluorescence intensity at the two wavelengths was calculated after subtraction of background fluorescence. Ratio levels were determined from groups of 20–40 individual cells and analyzed using MetaFluor (Universal Imaging Corp., West Chester, PA).

Electrophysiology—The whole cell patch clamp technique was used to record and measure LPA-induced effects on whole cell currents of B103 cells stably expressing LPA_4 receptor. The involvement of G_q in the modulations of cellular conductance was determined with stable LPA_4-B103 cells after infection with virus expressing the G_q minigene or empty vector that served as the control for minigene infection. Some LPA_4-B103

cells were treated overnight with PTX as described above. The extracellular solution (pH 7.4 with NaOH) contained the following: NaCl 145 mM, KCl 2.5 mM, $CaCl_2$ 1.5 mM, $MgSO_4$ 1.5 mM, HEPES 10 mM, dextrose 10 mM. LPA and vehicle were added to the bath by gravity perfusion at room temperature. Recording electrodes were fabricated and coated with dental periphery wax as described previously (22). Intracellular solution (pH 7.4) contained potassium gluconate 100 mM, KCl 25 mM, $MgCl_2$ 3 mM, $CaCl_2$ 0.483 mM, 1,2-bis(2-aminophenoxy)ethane-*N*,*N*,*N*′,*N*′-tetraacetic acid-K_4 1.0 mM, hemi-Na-HEPES 10 mM. The resistive whole cell configuration and data acquisition were achieved as described in Ref. 22. Cells were chosen for study if depolarization-activated peak inward current density was less than −30 pA/pF. During application of LPA (1 μM) or washout, cells were held at −50 mV, and the V_m value was stepped to −120 mV for 60 ms and ramped to +120 mV (at a rate of 1 mV/ms) every 2 s. All data are expressed in terms of the C_m value during stimulus application (current density).

Reverse Transcription-PCR—TRIzol reagent (Invitrogen) was used to extract RNA from cultured cells or tissues as described by the manufacturer. Five micrograms of total RNA was reverse-transcribed using Superscript II reverse transcriptase (Invitrogen). An equal quantity of cDNA was used to amplify LPA_4 and β-actin transcripts using the following conditions: 94 °C for 30 s, 60 °C for 45 s, and 72 °C for 45 s for a total of 30–35 cycles. The primers were used as follows: LPA_4, 5′-AGGCATGAGCACATTCTCTC-3′ (forward) and 5′-CAACCTGGGTCTGAGACTTG-3′ (reverse); β-actin, 5′-TGGAATCCTGTGGCATCCATGAAAC-3′ (forward) and 5′-TAAAACGCAGCTCAGTAACAGTCCG-3′ (reverse). The PCR products were analyzed by electrophoresis on a 1.2% agarose gel.

Northern Blot Analysis—A Northern blot (OriGene Technologies, Rockville, MD) containing 2 μg/lane of adult mouse poly(A)$^+$ RNA from several mouse tissues was probed with a random primed full-length ^{32}P-labeled mouse LPA_4 and human β-actin cDNA. DNA labeling was performed with the high prime DNA labeling kit (Roche Applied Science), and unincorporated nucleotides were separated out by passing the reaction mixture over a Sephadex G-50 quick spin column (Roche Applied Science). The Northern blot was then probed overnight in ULTRAhyb hybridization solution (Origen), washed several times, and analyzed using a PhosphorImager detection system.

Statistical Analysis of Data—Each data point was calculated from triplicate samples unless otherwise indicated. The data are presented ±S.D. Statistical analysis was performed by one-way analysis of variance and Dunnett's method, or Student's *t* test.

RESULTS

Mouse LPA_4 cDNA was epitope-tagged with hemagglutinin (HA) sequence at the 5′-end of the extracellular domain, and the construct was introduced into a murine leukemia, replication-deficient, bicistronic retroviral vector (Fig. 1*A*). This construct co-expresses tagged LPA_4 and EGFP, thus allowing for the identification of receptor expression in living and fixed cells by fluorescence microscopy.

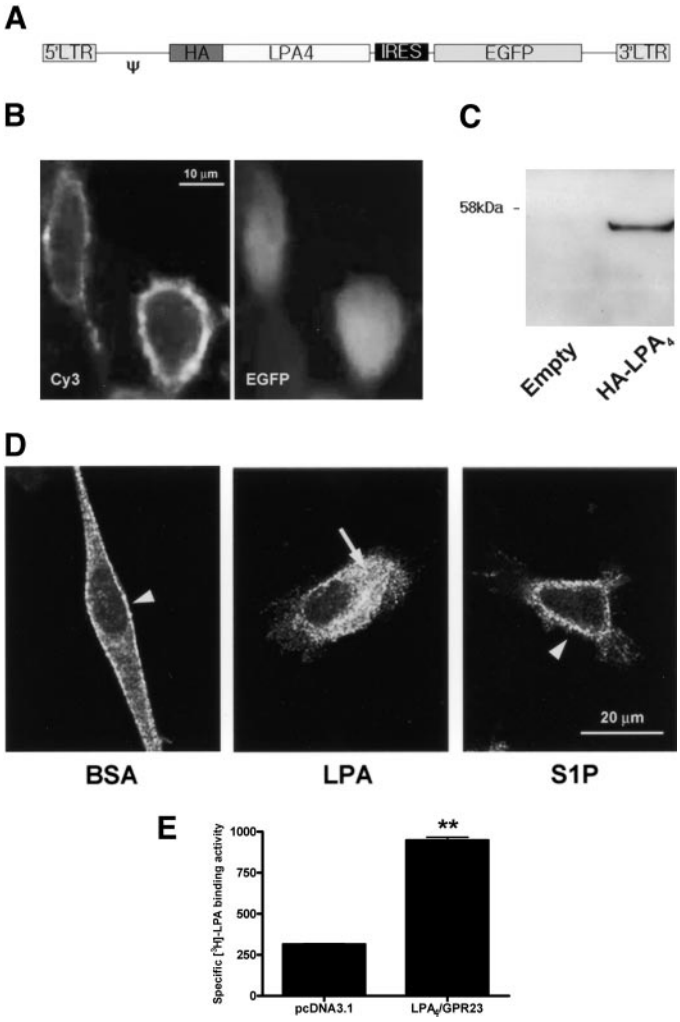

FIGURE 1. **LPA-mediated receptor internalization of LPA_4.** *A*, schematic of HA epitope-tagged LPA_4-retroviral expression vector construct. *LTR*, long terminal repeat; *ψ*, retrovirus packaging signal; *IRES*, internal ribosome entry site. *B*, surface expression of HA-LPA_4. HA-LPA_4-expressing B103 cells were immunostained with an anti-HA antibody and visualized with a Cy3-conjugated secondary antibody (Cy3), and these cells also expressed EGFP. *C*, Western blot assay of the membrane fraction isolated from B103 cells infected with the empty vector or HA-tagged LPA_4 retroviruses. *D*, LPA-mediated LPA_4 internalization. Infected B103 cells were treated with BSA, 1 μM LPA, or 1 μM sphingosine 1-phosphate (*SIP*) for 15 min after overnight serum starvation, and then immunostained as in *B*. An *arrowhead* shows surface expression of HA-LPA_4, and an *arrow* indicates internalization of the receptor. *E*, specific [^{3}H]LPA binding to cell membranes isolated from stable LPA_4-expressing RH7777 cells. Forty μg of membrane fraction from empty vector- or LPA_4-expressing cells was incubated with [^{3}H]LPA (4,042 dpm) for 30 min. Data are the mean ± S.D. (n = 3). **, $p < 0.01$ (using Student's *t* test) *versus* empty vector-expressing cells.

To demonstrate cell surface receptor gene expression, LPA_4-infected B103 cells were labeled with an anti-HA primary antibody, and receptor was visualized using Cy3-conjugated secondary antibody (Fig. 1*B*). Western blot analysis with an anti-HA antibody showed that the tagged receptor was of the expected size (Fig. 1*C*). To determine whether the LPA_4 receptor was indeed capable of binding to LPA, membranes were prepared from LPA_4-expressing cells and incubated with [^{3}H]LPA in the presence or absence of 10 μM cold LPA. Membranes prepared from LPA_4-expressing cells

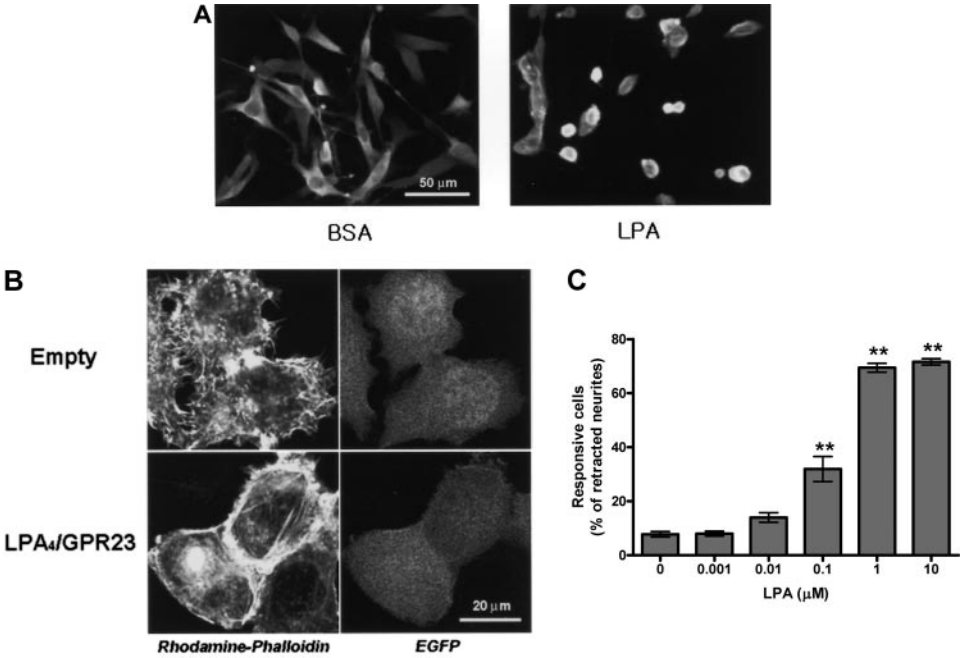

FIGURE 2. **LPA$_4$-mediated neurite retraction of B103 cells and stress fiber formation in RH7777 cells.** *A*, serum-starved LPA$_4$-expressing B103 cells were treated with fatty-acid free BSA (0.1%) or LPA (1 μM) for 30 min and then fixed and mounted on glass slides. *B*, empty vector- or LPA$_4$-expressing RH7777 cells were stimulated with 1 μM LPA for 30 min after overnight serum starvation. The cells were fixed and stained with rhodamine-phalloidin to detect actin stress fibers. *C*, quantification of LPA-induced neurite retraction for LPA$_4$-expressing B103 cells. The data are mean ± S.D. ($n = 3$). **, $p < 0.01$ (one-way analysis of variance) *versus* basal 0 μM LPA.

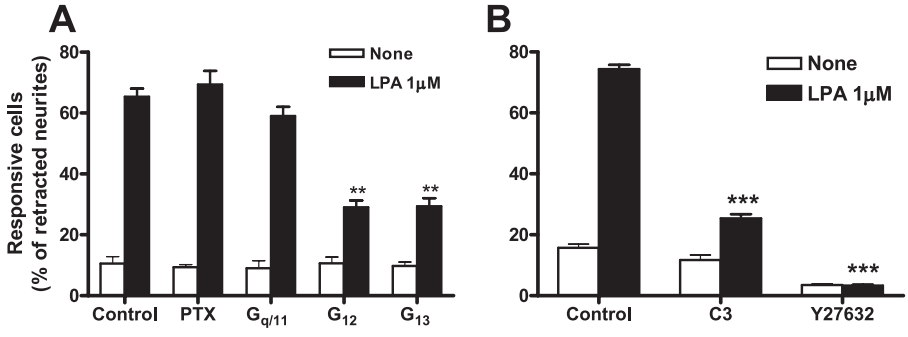

FIGURE 3. **G_{12}, G_{13}, and Rho signaling is involved in LPA$_4$-mediated neurite retraction of B103 cells.** *A*, LPA$_4$-expressing B103 cells were pretreated with PTX (200 ng/ml) overnight or infected with a G protein minigene 2 days prior to testing. Cells were fixed after treatment with 1 μM LPA for 30 min. *B*, LPA$_4$-expressing B103 cells were pretreated with C3 (10 μg/ml) for 24 h or pretreated with Y27632 (10 μM) for 45 min and then stimulated with 1 μM LPA for 30 min. Data are the mean ± S.D. ($n = 3$). **, $p < 0.01$; ***, $p < 0.001$ (one-way analysis of variance) *versus* control.

revealed statistically significant specific [^{3}H]LPA binding compared with membranes isolated from control cells (Fig. 1*E*).

G protein-coupled receptors typically undergo internalization during prolonged agonist exposure (28). We reasoned that if GPR23 is a physiologically relevant receptor for LPA but not other lysophospholipids, then LPA exposure would likely produce agonist-induced receptor internalization, whereas other ligands would not. We performed a standard internalization assay using B103 cells expressing HA-tagged LPA$_4$ and visualized LPA$_4$ localization with anti-HA immunolabeling and confocal microscopy. We found that receptor internalization occurred following LPA treatment but not with another lysophospholipid, sphingosine 1-phosphate (Fig. 1*D*). We noticed that during exposure to LPA the cells retracted their processes, a response observed for activation of heterologously expressed LPA$_{1,2,5}$ in B103 cells (see below). LPA$_4$ internalization was not a consequence of cell rounding because sphingosine 1-phosphate-induced retraction did not cause LPA$_4$ internalization.

We next sought to determine the signaling pathways mediating LPA$_4$-induced morphological changes in LPA$_4$-expressing B103 cells. A strong cell rounding response occurred within 30 min of LPA treatment (Fig. 2*A*). However, control vector-infected cells were unresponsive to LPA (data not shown). F-actin staining with rhodamine-phalloidin demonstrated stress fiber formation in LPA$_4$-expressing RH7777 cells (Fig. 2*B*) but not control cells. In B103 cells expressing LPA$_4$, LPA produced a concentration-dependent increase in the proportion of rounded cells (Fig. 2*C*), with ~70% of LPA$_4$-infected cells rounding after exposure to 1 μM LPA.

PTX and G-protein minigenes were used to determine which members of the heterotrimeric G-protein family are responsible for mediating the LPA-induced cell rounding of LPA$_4$-expressing cells (Fig. 3*A*). $G_{12/13}$ interacts with p115 RhoGEF, the Rho guanine nucleotide exchange factor (29, 30), activating the Rho signaling pathway to produce actin cytoskeleton rearrangement (31, 32). Using G_{12} and G_{13} minigenes to inhibit $G_{12/13}$ signaling, LPA-induced cell rounding was significantly reduced (Fig. 3*A*). Recently, $G_{q/11}$ has also been shown to activate a Rho-dependent pathway in $G_{12/13}$-deficient cells (33). However, blocking this pathway using a pan-$G_{q/11}$ minigene did not inhibit cell rounding in response to LPA (Fig. 3*A*). Blocking G_i signaling with PTX pretreatment (Fig. 3*A*) or G_s signaling using a G_s minigene (data not shown) also failed to inhibit LPA-induced cell rounding.

To test the involvement of Rho signaling in LPA receptor-mediated cell rounding, we used C3 toxin and Y27632 to inhibit Rho and Rho kinase, respectively. Similar to LPA$_1$- and LPA$_2$-induced Rho signaling-dependent cell rounding in infected cells (26), the cell rounding response in LPA$_4$-expressing B103 cells was inhibited by both C3 and Y27632 (Fig. 3*B*). Furthermore, LPA$_4$-mediated stress fiber formation in

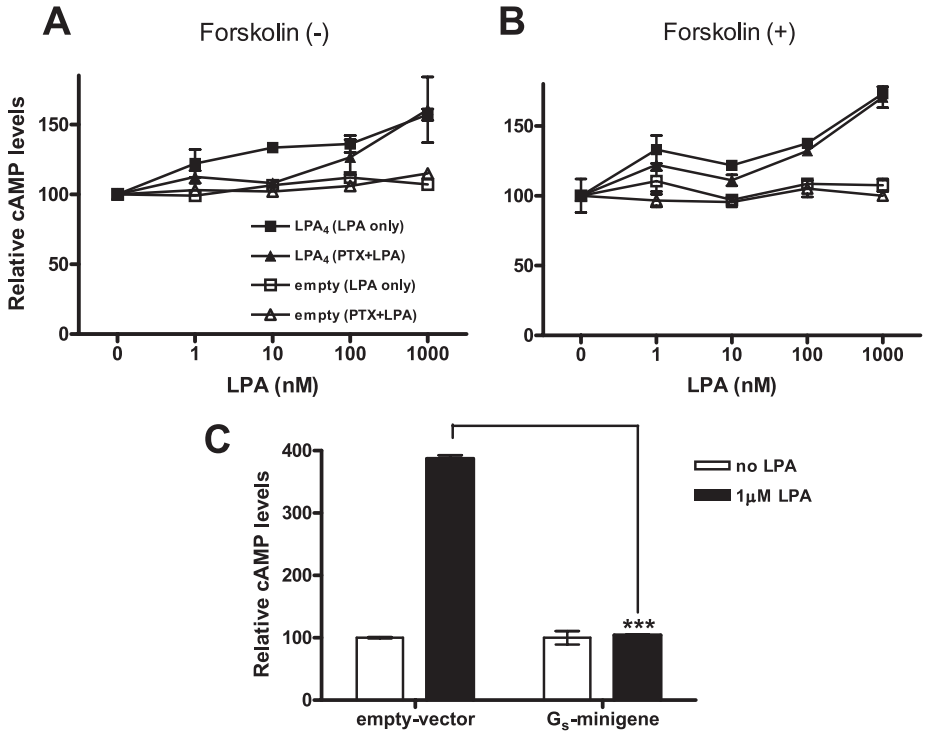

FIGURE 4. **LPA-induced intracellular cAMP accumulation.** *A*, concentration-response data for basal cAMP content in acutely LPA$_4$-infected B103 cells (■, PTX-untreated cells; ▲, PTX-treated cells (200 ng/ml)) and empty vector infected cells (□, PTX-untreated cells; △, PTX-treated cells) exposed to LPA in the presence of 0.5 mM 3-isobutyl-1-methylxanthine. *B*, effect of forskolin on cAMP accumulation in LPA$_4$-infected B103 cells. LPA was added to cells in the presence of 5 μM forskolin in the same manner as in *A*, and basal levels were about 15 times higher than forskolin-free conditions. *C*, cAMP accumulation in stably transfected LPA$_4$-expressing B103 cells infected with control or G$_s$ minigene retrovirus after treatment with 1 μM LPA under forskolin-free conditions. About 50% of the cells expressed LPA$_4$ through acute retroviral infection in *A* and *B*, whereas stably expressing cells were used for the experiments employing minigene retroviruses.

RH7777 cells was completely blocked by C3 and Y27632 treatment (data not shown).

Because all known lysophospholipid GPCRs can influence cAMP levels (14), we analyzed cAMP levels in LPA$_4$-expressing B103 cells after LPA exposure. LPA increased intracellular cAMP levels in LPA$_4$-expressing cells either in the absence or presence of forskolin (5 μM) (Fig. 4, *A* and *B*). Because intracellular cAMP levels are regulated by G$_s$ α subunit as well as G protein $\beta\gamma$ subunits, (34, 35), we tested whether G$_s$ was responsible for LPA$_4$-mediated cAMP induction using a G$_s$ minigene (Fig. 4*C*). LPA$_4$-mediated cAMP accumulation was completely blocked by a G$_s$ minigene (Fig. 4*C*). Thus, the LPA$_4$ receptor coupling to G$_s$ activates adenylyl cyclase to increase intracellular cAMP levels.

We next sought to determine the signaling pathway(s) mediating LPA$_4$-induced calcium mobilization in B103 cells (20). In LPA$_4$-expressing B103 cells (Fig. 5*A*), but not vector control cells (Fig. 5*B*), LPA significantly elevated intracellular calcium levels. The response appears to desensitize in the continued presence of LPA. Interestingly, when cells were pretreated with PTX or expressed a G$_q$ minigene for at least 2 days, LPA-induced intracellular calcium levels were partially reduced (Fig. 5, *C* and *D*). When cells were transfected with a G$_q$ minigene and treated with PTX, the calcium response was nearly completely abolished. These results indicate that PTX-sensitive G proteins and G$_q$ are essential for intracellular calcium mobilization in LPA$_4$-expressing cells. It is well established that G$\beta\gamma$ subunits of PTX-sensitive G$_i$ proteins activate phospholipase Cβ (36).

To further investigate intracellular signaling pathways modulated by LPA$_4$ receptor activation, we used a "resistive" whole cell patch clamp technique (22) to determine whether LPA could influence ion channel function through LPA$_4$ signaling. LPA (100 nM (not shown) and 1 μM) activated a transient conductance in stably transfected LPA$_4$-expressing cells that was not observed in cells transfected with empty vector (Fig. 6*A*). Whole cell currents induced by LPA$_4$ receptor activation had a latency of 31 $\pm$ 4 s (n = 18) consistent with a GPCR-mediated effect and a reversal potential of -7 ± 2 mV (n = 17), suggesting enhancement of nonselective cation channel activity (Fig. 6*B*). LPA-CI μM induced current density was -1.8 ± 0.3 pA/pF and $+2.5 \pm 0.4$ pA/pF at -120 and $+120$ mV, respectively (n = 16). Stable LPA$_4$-B103 transfectants were used to identify G protein signaling pathways involved in activation of the putative nonselective cation conductance (Fig. 6*C*). PTX pretreatment decreased ramp-induced currents at -120 and $+120$ mV by 42 and 45%, respectively (Fig. 6*C*), and PTX together with expression of a G$_q$ minigene substantially reduced LPA-induced currents even further to 3 and 6%, respectively (Fig. 6*C*). Thus, activation of LPA-induced nonselective cation conductance by G proteins had a similar pharmacological profile as the LPA-induced intracellular calcium response.

We next performed Northern blot and RT-PCR analysis to assess the tissue expression of LPA$_4$ (Fig. 7). LPA$_4$ mRNA expression was detected in heart, skin, thymus, bone marrow, mouse embryonic fibroblast, embryonic brain, and embryonic stem cells (Fig. 7).

DISCUSSION

A critical aspect of understanding receptor-mediated lysophospholipid signaling has been the identification of receptors that meet clear, unambiguous criteria for receptor function, combined with independent confirmation of the proposed identity. In the lysophospholipid receptor field, multiple instances of initial receptor mis-identification have occurred, most notably the following: OGR1 as a sphingosylphosphorylcholine receptor (38), GPR4 as a lysophosphatidylcholine and sphingosylphosphorylcholine receptor

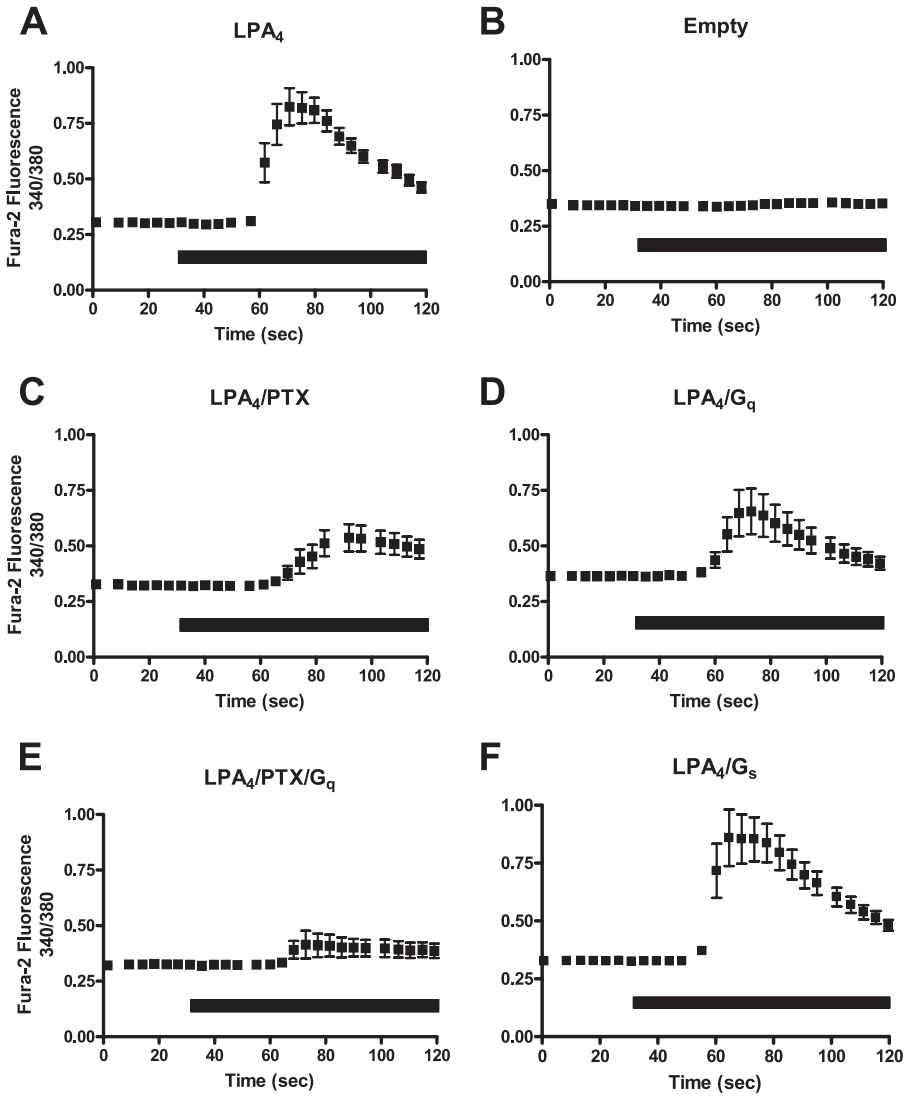

FIGURE 5. **LPA causes intracellular calcium mobilization in LPA$_4$-expressing B103 cells.** *A*, 1 μM LPA induced intracellular calcium mobilization in LPA$_4$-infected B103 cells. *B*, no effect was observed in control cells expressing empty vector. *C*, LPA$_4$-infected cells were pretreated with PTX (200 ng/ml) overnight prior to LPA treatment and calcium imaging. *D*, LPA$_4$-expressing B103 cells were infected with retrovirus expressing G$_q$ minigene. *E*, G$_q$-infected LPA$_4$-expressing cells were pretreated with PTX (200 ng/ml). These experiments were repeated 4–5 times independently. *F*, G$_s$-infected LPA$_4$-expressing cells were similar to control. The time required for solution to traverse the delivery tubing and reach the recording chamber was about 20–30 s.

(39), G2A as an lysophosphatidylcholine receptor (40, 41), and mammalian PSP24s as an LPA receptor (42). Our assessment here of LPA$_4$ completely supports its initial identification (20), including concentration-dependent LPA-induced responsivity for several end points, along with receptor internalization and [^{3}H]LPA binding to heterologously expressed LPA$_4$ membrane fractions.

Five novel aspects of LPA$_4$ functionality emerged from the present analysis. First, and perhaps most notable, was the finding that calcium mobilization occurs via both G$_q$- and a G$_{i/o}$-mediated pertussis toxin-sensitive pathway. This contrasts with previous studies on LPA$_{1-3}$ (7, 10, 14, 17, 26) and LPA$_5$ (22), which identified LPA-dependent calcium mobilization via a G$_q$ pathway, with no detectable PTX-sensitive component. It also indicates the paradoxical activation of both G$_i$ and G$_s$ within the same cell line, with G$_s$ being dominant, at least with respect to adenylyl cyclase activation. This activity is consistent with previous reports in which phosphorylation of the β_2-adrenergic receptor by cAMP-dependent protein kinase is proposed to switch its coupling specificity from G$_s$ to G$_i$ (43). Receptor-dependent activation of G$_i$ could thus release sufficient G$\beta\gamma$ to activate phospholipase Cβ (36). Hence, the G$_s$/G$_i$ switching model is a potential mechanism to explain the ability of LPA$_4$ to activate both G$_s$ and G$_i$.

Second, activation of LPA$_4$ evoked a nonselective cation conductance through similar G protein-mediated pathways as those that modulate calcium signaling. This activity may contribute to the nonselective cation conductance seen in physiological responses of primary neuroprogenitor cells from the embryonic cerebral cortex (46).

Third, LPA$_4$ stimulation induced G$_{12/13}$-mediated Rho activation producing neurite retraction and stress fiber formation. These functions are shared with all other LPA receptors except LPA$_3$ (26). This may have relevance to embryonic brain development, where LPA signaling alters the shapes and positions of young neuroblasts (8, 44, 45).

Fourth, G$_s$ produced increased cAMP levels during activation of LPA$_4$ in B103 cells. Other potential mechanisms for increasing cAMP have been reported, including G $\beta\gamma$ subunit activity that is independent of G$_s$ α subunit (34, 35). It is likely that this mechanism, if involved, plays only a minor role because blocking G$_s$ activity with the minigene approach virtually abolished LPA-induced cAMP production. Thus, receptor-mediated LPA signaling can raise levels of intracellular cAMP via two different GPCRs, LPA$_4$ and LPA$_5$ (22), complementing the cAMP-attenuating activities of LPA$_{1-3}$ (14, 26).

Fifth, this is the first demonstration of LPA$_4$ gene expression in the mouse that reveals the highest levels in heart, skin, and thymus and contrasts somewhat with the lower expression levels observed in human tissues (20). In addition, gene expression was identified in multiple new tissues, including embryonic brain, bone marrow, and embryonic stem cells.

In a recent publication it has been reported that deletion of the autotaxin gene in mice leads to early embryonic lethality because of a defect in blood vessel formation (47). This demonstrates an essential function for autotaxin in normal develop-

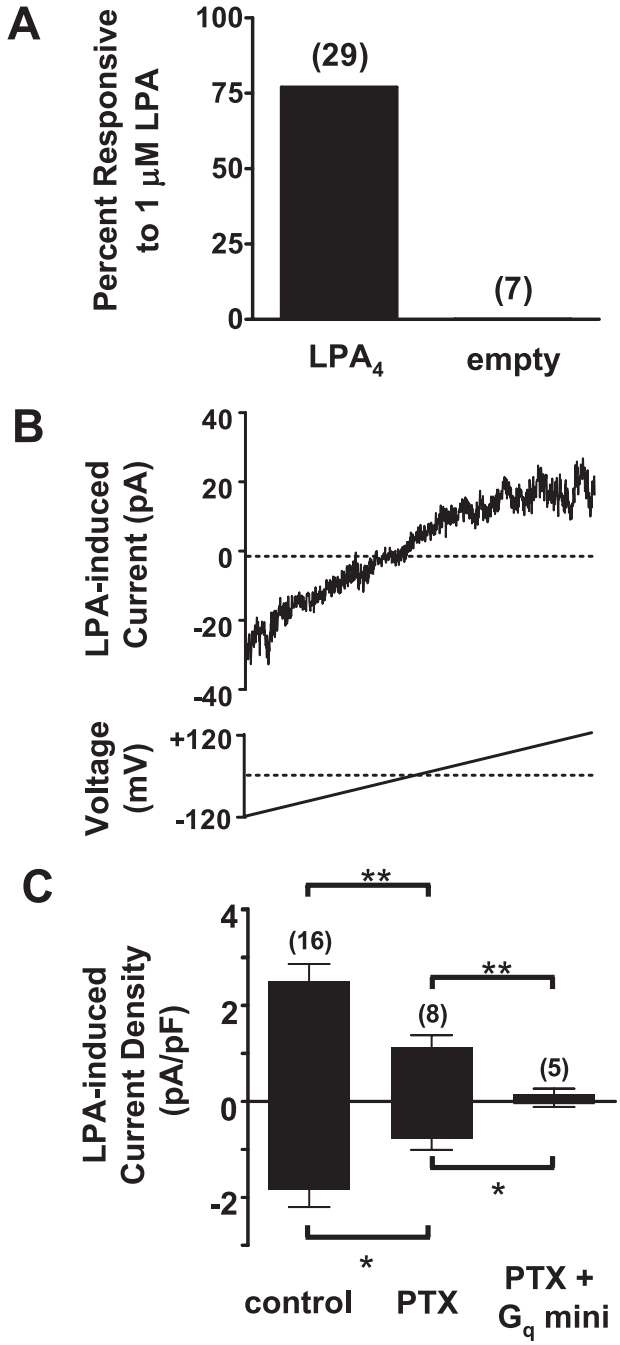

FIGURE 6. **LPA-evoked currents in LPA$_4$-expressing B103 cells.** *A,* about 75% of LPA$_4$-expressing B103 cells were responsive to LPA (1 μM); no LPA-induced conductance changes were detected within 90 s in cells infected with empty vector. The total number of cells tested is shown *above each bar*. *, $p < 0.01$, χ^2 analysis. All cells expressed outward currents and fast transient voltage-gated inward peak currents < -30 pA/pF. *B,* exposure of LPA$_4$-expressing B103 cells to LPA (1 μM) elicited a current that reversed near 0 mV, consistent with the activation of a nonselective cation conductance. The voltage protocol is indicated *below* the current trace. The *dotted lines* indicate 0 pA (*top*) and 0 mV (*bottom*). *C,* whole cell current density at +120 mV (positive values) and −120 mV (negative values) induced by 1 μM LPA in control (*left bar*), PTX-treated (*center bar*), and PTX-treated-G$_q$ minigene-expressing LPA$_4$-expressing B103 cells (*right bar*). The control cells for G$_q$-minigene-infected cells were EGFP-positive LPA$_4$-expressing B103 cells infected with empty minigene virus vector. *, $p < 0.05$; **, $p < 0.01$ (Student's *t* test).

ment that most likely involves LPA signaling mechanisms (although nucleotide pyrophosphatase/phosphodiesterase functions cannot be excluded) (37, 48, 49). The existence of five

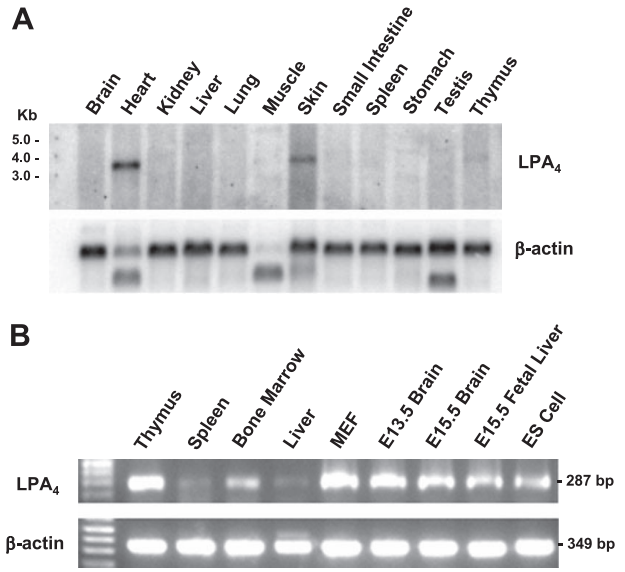

FIGURE 7. **LPA$_4$ expression in mouse tissues.** *A,* Northern blot of tissue poly(A)$^+$ RNA (2 μg/lane) from 6- to 8-week-old BALB/c adult mice. A random primed ^{32}P-labeled probe was used as described under "Materials and Methods." *B,* RT-PCR of total RNAs from various tissues using LPA$_4$ primers as described under "Materials and Methods." β-Actin was used as a loading control. *MEF,* murine embryonic fibroblasts; *ES*, mouse embryonic stem cells.

confirmed LPA receptors makes it probable that most if not all LPA receptors will need to be deleted to recapitulate the autotaxin-null phenotype, consistent with the partially viable phenotype of mice deficient for one or two LPA receptors (10, 11). The biological roles of LPA$_4$ in concert with the other four LPA receptors remain to be determined.

Acknowledgments—We thank Drs. Brigitte Anliker and Eric Birgbauer for advice and assistance.

REFERENCES

1. Moolenaar, W. H. (1995) *J. Biol. Chem.* **270,** 12949–12952
2. Moolenaar, W. H., Kranenburg, O., Postma, F. R., and Zondag, G. C. (1997) *Curr. Opin. Cell Biol.* **9,** 168–173
3. van Corven, E. J., Groenink, A., Jalink, K., Eichholtz, T., and Moolenaar, W. H. (1989) *Cell* **59,** 45–54
4. van der Bend, R. L., de Widt, J., van Corven, E. J., Moolenaar, W. H., and van Blitterswijk, W. J. (1992) *Biochem. J.* **285,** 235–240
5. Amano, M., Chihara, K., Kimura, K., Fukata, Y., Nakamura, N., Matsuura, Y., and Kaibuchi, K. (1997) *Science* **275,** 1308–1311
6. Moolenaar, W. H. (1995) *Curr. Opin. Cell Biol.* **7,** 203–210
7. Contos, J. J., Ishii, I., and Chun, J. (2000) *Mol. Pharmacol.* **58,** 1188–1196
8. Fukushima, N., Weiner, J. A., Kaushal, D., Contos, J. J., Rehen, S. K., Kingsbury, M. A., Kim, K. Y., and Chun, J. (2002) *Mol. Cell. Neurosci.* **20,** 271–282
9. Ye, X., Ishii, I., Kingsbury, M. A., and Chun, J. (2002) *Biochim. Biophys. Acta* **1585,** 108–113
10. Contos, J. J., Fukushima, N., Weiner, J. A., Kaushal, D., and Chun, J. (2000) *Proc. Natl. Acad. Sci. U. S. A.* **97,** 13384–13389
11. Contos, J. J., Ishii, I., Fukushima, N., Kingsbury, M. A., Ye, X., Kawamura, S., Brown, J. H., and Chun, J. (2002) *Mol. Cell. Biol.* **22,** 6921–6929
12. Gardell, S. E., Dubin, A. E., and Chun, J. (2006) *Trends Mol. Med.* **12,** 65–75
13. Fukushima, N., Ishii, I., Contos, J. J., Weiner, J. A., and Chun, J. (2001) *Annu. Rev. Pharmacol. Toxicol.* **41,** 507–534
14. Ishii, I., Fukushima, N., Ye, X., and Chun, J. (2004) *Annu. Rev. Biochem.* **73,** 321–354

15. Ye, X., Hama, K., Contos, J. J., Anliker, B., Inoue, A., Skinner, M. K., Suzuki, H., Amano, T., Kennedy, G., Arai, H., Aoki, J., and Chun, J. (2005) *Nature* **435,** 104–108
16. Inoue, M., Rashid, M. H., Fujita, R., Contos, J. J., Chun, J., and Ueda, H. (2004) *Nat. Med.* **10,** 712–718
17. Hecht, J. H., Weiner, J. A., Post, S. R., and Chun, J. (1996) *J. Cell Biol.* **135,** 1071–1083
18. An, S., Bleu, T., Hallmark, O. G., and Goetzl, E. J. (1998) *J. Biol. Chem.* **273,** 7906–7910
19. Bandoh, K., Aoki, J., Hosono, H., Kobayashi, S., Kobayashi, T., Murakami-Murofushi, K., Tsujimoto, M., Arai, H., and Inoue, K. (1999) *J. Biol. Chem.* **274,** 27776–27785
20. Noguchi, K., Ishii, S., and Shimizu, T. (2003) *J. Biol. Chem.* **278,** 25600–25606
21. Kotarsky, K., Boketoft, A., Bristulf, J., Nilsson, N. E., Norberg, A., Hansson, S., Sillard, R., Owman, C., Leeb-Lundberg, F. L., and Olde, B. (2006) *J. Pharmacol. Exp. Ther.* **318,** 619–628
22. Lee, C. W., Rivera, R., Gardell, S., Dubin, A. E., and Chun, J. (2006) *J. Biol. Chem.* **281,** 23589–23597
23. Fukushima, N., Kimura, Y., and Chun, J. (1998) *Proc. Natl. Acad. Sci. U. S. A.* **95,** 6151–6156
24. Pear, W., Scott, M., and Nolan, G. (1997) *Methods in Molecular Medicine: Gene Therapy Protocols*, pp. 41–57, Humana Press Inc., Totowa, NJ
25. Gilchrist, A., Li, A., and Hamm, H. E. (2002) *Sci. STKE 2002,* PL1
26. Ishii, I., Contos, J. J., Fukushima, N., and Chun, J. (2000) *Mol. Pharmacol.* **58,** 895–902
27. Chun, J., Contos, J. J., and Munroe, D. (1999) *Cell Biochem. Biophys.* **30,** 213–242
28. Ferguson, S. S. (2001) *Pharmacol. Rev.* **53,** 1–24
29. Hart, M. J., Jiang, X., Kozasa, T., Roscoe, W., Singer, W. D., Gilman, A. G., Sternweis, P. C., and Bollag, G. (1998) *Science* **280,** 2112–2114
30. Kozasa, T., Jiang, X., Hart, M. J., Sternweis, P. M., Singer, W. D., Gilman, A. G., Bollag, G., and Sternweis, P. C. (1998) *Science* **280,** 2109–2111
31. Sah, V. P., Seasholtz, T. M., Sagi, S. A., and Brown, J. H. (2000) *Annu. Rev. Pharmacol. Toxicol.* **40,** 459–489
32. Seasholtz, T. M., Majumdar, M., and Brown, J. H. (1999) *Mol. Pharmacol.* **55,** 949–956
33. Vogt, S., Grosse, R., Schultz, G., and Offermanns, S. (2003) *J. Biol. Chem.* **278,** 28743–28749
34. Tang, W. J., and Gilman, A. G. (1991) *Science* **254,** 1500–1503
35. Federman, A. D., Conklin, B. R., Schrader, K. A., Reed, R. R., and Bourne, H. R. (1992) *Nature* **356,** 159–161
36. Clapham, D. E. (1995) *Cell* **80,** 259–268
37. Hama, K., Aoki, J., Fukaya, M., Kishi, Y., Sakai, T., Suzuki, R., Ohta, H., Yamori, T., Watanabe, M., Chun, J., and Arai, H. (2004) *J. Biol. Chem.* **279,** 17634–17639
38. Xu, Y., Zhu, K., Hong, G., Wu, W., Baudhuin, L. M., Xiao, Y., and Damron, D. S. (2006) *Nat. Cell Biol.* **8,** 299
39. Zhu, K., Baudhuin, L. M., Hong, G., Williams, F. S., Cristina, K. L., Kabarowski, J. H. S., Witte, O. N., and Xu, Y. (2005) *J. Biol. Chem.* **280,** 43280
40. Witte, O. N., Kabarowski, J. H., Xu, Y., Le, L. Q., and Zhu, K. (2005) *Science* **307,** 206
41. Murakami, N., Yokomizo, T., Okuno, T., and Shimizu, T. (2004) *J. Biol. Chem.* **279,** 42484–42491
42. Kawasawa, Y., Kume, K., Izumi, T., and Shimizu, T. (2000) *Biochem. Biophys. Res. Commun.* **276,** 957–964
43. Daaka, Y., Luttrell, L. M., and Lefkowitz, R. J. (1997) *Nature* **390,** 88–91
44. Fukushima, N., Weiner, J. A., and Chun, J. (2000) *Dev. Biol.* **228,** 6–18
45. Kingsbury, M. A., Rehen, S. K., Contos, J. J., Higgins, C. M., and Chun, J. (2003) *Nat. Neurosci.* **6,** 1292–1299
46. Dubin, A. E., Bahnson, T., Weiner, J. A., Fukushima, N., and Chun, J. (1999) *J. Neurosci.* **19,** 1371–1381
47. van Meeteren, L. A., Ruurs, P., Stortelers, C., Bouwman, P., van Rooijen, M. A., Pradere, J. P., Pettit, T. R., Wakelam, M. J., Saulnier-Blache, J. S., Mummery, C. L., Moolenaar, W. H., and Jonkers, J. (2006) *Mol. Cell. Biol.* **26,** 5015–5022
48. Umezu-Goto, M., Kishi, Y., Taira, A., Hama, K., Dohmae, N., Takio, K., Yamori, T., Mills, G. B., Inoue, K., Aoki, J., and Arai, H. (2002) *J. Cell Biol.* **158,** 227–233
49. Tokumura, A., Majima, E., Kariya, Y., Tominaga, K., Kogure, K., Yasuda, K., and Fukuzawa, K. (2002) *J. Biol. Chem.* **277,** 39436–39442